Protein In-Cell NMR in *Escherichia coli*

Christopher O. Barnes

A thesis submitted to the faculty of the University of North Carolina at Chapel Hill in partial fulfillment of the requirements for the degree of Masters of Arts in the Department of Chemistry.

Chapel Hill
2010

Approved by

Advisor: Professor Gary J. Pielak, Ph.D.

Reader: Professor Todd L. Austell, Ph.D.

Reader: Professor Matthew R. Redinbo, Ph.D.

Abstract

Christopher O. Barnes: Protein In-Cell NMR in *Escherichia coli*
(Under the direction of Professor Gary J. Pielak, Ph.D.)

The inside of the cell is a crowded and complex environment that is impossible to duplicate by studying proteins and other molecules in dilute solution. The effects of macromolecular crowding are potentially important to all cellular functions, but until recently studies have been conducted mostly in dilute solution. In-cell Nuclear Magnetic Resonance (NMR) spectroscopy is becoming an important tool in studying proteins under physiologically relevant conditions. In some instances, however, protein signals from leaked protein are seen in the supernatant surrounding the in-cell slurry. I examined how expression levels contribute to protein leakage. I also describe a device and system that provides a controlled environment for NMR experiments in living cells. I have utilized this device to study the expression of the natively disordered protein α-synuclein, inside *Escherichia coli*. In the future, we hope to make progress in using this device to study proteins in eukaryotic cells with NMR.

Dedication

To my parents Will and Vanessa, my siblings Alex and Dominique, and my entire UNC family…thanks for the love, support, guidance, and inspiration you've given me over the past six years of my life.

Acknowledgements

Thank you Lord for placing so many wonderful, caring and supporting people in my life during my time here at UNC. To Gary Pielak, my advisor and friend, thank you for all the opportunities and wisdom you provided. I can never repay you for molding me into the scientist I am today, and for that I am truly thankful. To my committee members, Drs. Matt Redinbo and Todd Austell, thank you for your countless advice, guidance, and time. To my best friend and colleague, Naima G. Sharaf, thank you for your love and support, in addition to pushing me to reach my potential as a scientist, even on national holidays. To Dr. Lisa Charlton, thank you for making science interesting and for putting up with all of my questions over the last four years. To past and present members of the most awesomest group around, thank you for making each day memorable and endearing. To my family, coaches and Dr. Kathy Wood, thank you for listening and providing words of encouragement when I was ready to give up on science. To all my Tar Heel teammates, friends, and family, thanks for all the good times and memories, you all were truly my outlet. Lastly, I'll end with this: I'm a Tar Heel born, I'm a Tar Heel bred, and when I die I'm a Tar Heel dead. So it's rah rah Carolina, 'lina, rah, rah, Carolina, 'lina, rah, rah, Carolina, 'lina, GO TO HELL DUKE!!! I'm a Tar Heel for Life!!!

Table of Contents

List of Tables

List of Figures

List of Abbreviations and Symbols

2D	two-dimensional
A_{600}	Absorbance at 600 nm
CEC	circulating encapsulated cells
CI2	chymotrypsin inhibitor 2
EDTA	ethylenediaminetetraacetic acid
g	standard gravity
h	hour
HMQC	heteronuclear multiple quantum correlation
HSQC	heteronuclear single quantum correlation
Hz	Hertz
IPTG	isopropyl β-D-1-thiogalactopyranoside
kDa	kilodalton
kV	kilovolt
min	minute
mg	milligram
mL	milliliter
mM	millimolar
mm	millimeter
MWCO	molecular weight cut off

nm	nanometer
NMR	nuclear magnetic resonance
OD	outer diameter
PAGE	polyacrylamide gel electrophoresis
PBS	phosphate buffered saline
Rpm	revolutions per minute
SDS	sodium dodecyl sulfate
SOFAST	band-selective optimized flip-angle short transient
w/v	weight/volume
v:v	volume:volume

1 Introduction

1.1 Implications of a crowded cellular environment

The inside of the cell is a complex entity whose characteristics are hard to define and difficult to emulate *in vitro*. Macromolecules comprise at least 30% of the cell's volume, while water comprises the other 50-70% depending on extracellular conditions [1]. Macromolecular concentrations, however, can be greater than 300 g/L within the cell [2], and where crowding can affect many cellular functions. In comparison, macromolecular concentrations are <10 g/L for experiments carried out *in vitro*. For this reason, scientist have long been interested in studying proteins and polysaccharides in concentrated systems [3].

Recent studies that attempt to mimic the cellular environment have shown significant effects on protein stability, diffusion, structure, association, and metabolism. The effects of macromolecular crowding on protein association and dissociation are debatable. Crowding has been shown to effect in the formation of enzymatic complexes [4]. Other work, however, has show that the effects of crowding on the association of protein complexes can be equal to that found in dilute solution [5]. Regardless, the complex formation promotes metabolite channeling, which is considered key to cellular function [6]. The crowded cellular environment also hinders protein diffusion in the cytoplasm of *Escherichia coli* compared to experiments in dilute solution [7-11].

Excluded volume theory helps explain the effects of macromolecular crowding. This theory states that two molecules cannot occupy the same space at the same time, thus making some volume inaccessible to the protein. The resulting steric exclusion causes globular proteins to favor the compact state by destabilizing the more open denatured state [12, 13]. Through the use of amide-proton NMR exchange experiments, macromolecular crowding, by synthetic polymers, has been shown to stabilize a globular protein [14, 15]. Conversely, other studies report minimal increases, or even a decrease in protein stability [16, 17]. In addition, crowding can affect other structural properties like aggregation, shape and folding dynamics or functional properties like ligand binding [16, 18].

The works cited above are only a taste of data collected in recent years. Nevertheless, the conclusion is clear: the effects of macromolecular crowding should be an essential consideration when studying proteins and other macromolecules *in vitro*. These experiments, however, are imperfect because most crowding agents studied so far (i.e. synthetic polymers) are inert and homogenous, conditions unlike the inside of a cell. Therefore, there exists a need to observe the behavior of macromolecules within the cell. In-cell Nuclear Magnetic Resonance (NMR) spectroscopy may be the novel tool to achieve this goal.

1.2 Protein in-cell NMR

In-cell NMR is a technique that can provide atomic level information about isotopically-enriched macromolecules inside cells. Initial in-cell NMR experiments quantified rotational mobility of enzymes in yeast, by incorporating 5-fluorotryptophan

and using ^{19}F NMR [19]. This technique was later adapted to incorporate ^{15}N and eventually ^{13}C active nuclei into proteins and other macromolecules [20, 21].

The Pielak lab was the first to investigate intrinsically disordered proteins in cells. The protein, Flgm, showed a disappearance in crosspeaks corresponding to the C-termini suggesting a gain in structure for this region of the protein [22]. Another protein, α-synuclein, was shown to be protected in the periplasm from a conformational change seen in dilute solution at 35 °C [23]. In brief, other studies have shown that in-cell NMR can be used to study structural changes in proteins, protein-ligand binding, and protein-protein interactions in *E. coli* [24]. Progress has also been made in using in-cell NMR in eukaryotic systems [25, 26]. These results show the need to study proteins in physiologically relevant environments.

Nevertheless, no tool is perfect. One disadvantage of NMR spectroscopy is its low sensitivity. Selective isotopic enrichment or labeling of the targeted species with an NMR active nucleus (e.g., ^{15}N, ^{13}C or ^{19}F) is one way around this problem. Serber *et al.* suggest that the minimum concentration of the protein under study should be at least ~150 μM for ^{15}N enrichment, ~50 μM for ^{13}C enrichment, or ~50-100 μM for ^{19}F enrichment [20, 27]. Therefore, the target protein must be overexpressed or high concentrations must be introduced into the cell by other means. Nonetheless, ^{15}N enrichment and overexpression are no guarantee of the ability to collect high resolution NMR data for globular proteins inside *E. coli* [27]. In addition, certain proteins leak from cells resulting in invalid in-cell NMR data [27-29]. One last drawback to high-resolution in-cell NMR experiments is the need for highly dense cell samples to overcome the

inherit insensitivity of NMR. Higher cell densities, however, results in decreased cell viability, especially for eukaryotic systems.

The research I present addresses these disadvantages. I attempt to answer two questions: does overexpression lead to protein leakage, and can a system be developed to maintain cell viability, while preserving sensitivity? The results of my research will be presented in the subsequent chapters. The last chapter summerizes my results and describes progress in applying our system to eukaryotic cells.

2 *Escherichia coli* expression levels and in-cell protein NMR

2.1 Introduction

The cellular environment is complex, with macromolecular concentrations approaching 400 g/L [2]. Most proteins are studied outside cells in dilute solution with macromolecular concentrations of 10 g/L or less. There can be discrepancies when studying proteins in dilute solution compared to the crowded cellular environment [14, 17, 18, 23, 28]. There is, therefore, a need to study proteins under physiologically relevant conditions.

^{15}N enrichment and overexpression alone are often insufficient to obtain high quality in-cell NMR spectra of the protein of interest in *Escherichia coli* [27]. Specifically, the intracellular environment causes resonances to broaden beyond the detection limit in two-dimensional NMR spectra. This situation makes it likely that leaked proteinl will cause artifactual results [24, 27, 29].

Here, we investigate the connection between overexpression and leakage. We studied four proteins. One protein α-synuclein, is a 14.4 kDa intrinisically disordered protein that has been observed in both the periplasm and cytoplasm of the cell [11, 23]. HdeA, a 11.8 kDa globular dimer, is exclusively found in the periplasm [23, 30]. We also studied chymotrypsin inhibitor 2 (CI2), a 7.4 kDa protein, normally found in the cytoplasm but has also been shown to localize in the periplasmic space [27, 31], and ubiquitin, a 8.5 kDa well studied globular protein [31, 32].

2.2 Materials and Methods

2.2.1 Cultivation of *E. coli* for in-cell NMR

The pET-21 c(+) plasmid containing the HdeA gene was transformed into *E. coli* Bl-21 (DE3) Gold cells (Strategene). Plasmid containing cells were selected with 0.1 mg/mL ampicillin. A 5 mL overnight culture was grown from a single colony. The overnight culture was used to inoculate a 100 mL culture of M9 minimal media [20] containing 1 g/L $^{15}NH_4Cl$. The culture was incubated at 37°C in a rotary shaker (225 rpm, New Burnswick Scientific, Model I-26). After reaching an absorbance at 600 nm (A_{600}) of 0.6-0.8, the culture was induced with isopropyl β-D-thiogalactopyranoside (IPTG) to a final concentration of 1 mM. The culture was placed in the rotary shaker (225 rpm) at 37°C. After 1.5 h, a 50 mL aliquot was pelleted using a swinging bucket centrifuge (Sorvall RC-3B, H6000A rotor) at 1600*g* for 20 min at 4°C. The pellet was resuspended in 1 mL of Phosphate Buffered Saline (PBS, 3.2 mM Na_2HPO_4, 0.5 mM KH_2PO_4, 1.3 mM KCl, 135 mM NaCl, pH 7.4). The other 50 mL was allowed to express protein for 3 h before processing as described above.

Immediately after obtaining in-cell NMR spectra, cells were pelleted by centrifugation (Eppendorf model 5418) at 2000*g* for 10 min at room temperature. The supernatant was removed for NMR experiments. The resulting cell pellet was

resuspended in 1 mL lysis buffer (50 mM Tris, 150 mM NaCl, pH 8.0) and sonicated (Branson Ultrasonics, Fischer Scientific) for 1 min with a duty cycle of 4 s on 2 s off. The lysate was harvested by centrifugation (Eppendorf model 5418) at 14,000*g* for 5 min at room temperature.

2.2.2 Intracellular Protein Concentrations

The pET-21c (+), pT7-7, pET-21 and pET-46 plasmids containing the genes for HdeA, α-synucelin, chymotrypsin inhibitor 2 (CI2), and ubiquitin respectively, were transformed into *E. coli* Bl-21 (DE3) Gold cells (Strategene). Plasmid containing cells for HdeA, α-synucelin and ubiquitin were selected with 0.1 mg/mL ampicillin. Plasmid containing cells for CI2 were selected with 0.06 mg/mL kanamycin. Cells were grown and proteins expressed as described above. After 1.5, 2 and 3 h of expression an aliquot was diluted with PBS so that the A_{600} was 1.0, which equals 6.0 x 10^8 cells [33]. A 1 mL aliquot was removed from the diluted samples and centrifuged (Eppendorf model 5418) at 14,000*g* for 2 min at room temperature. The concentrations were calculated as described by a previous study [11].

2.2.3 NMR

Data were acquired at the UNC Biomeolcular NMR facility on a Varian Inova 600 MHz NMR spectrometer. Data were processed and visualized with NMRpipe and NMRviewJ, respectively [34, 35].

Samples for simple in-cell NMR experiments comprised 90:10 (v:v) mixture of resuspended cells: D_2O in a standard 5 mm NMR tube. ^{1}H-^{15}N HMQC (ref) spectra were acquired at 37^{o}C with a 5 mm Varian Triax triple resonance probe (^{1}H sweep width: 11990.40 Hz; ^{15}N sweep width: 2100 Hz, 32 transients, 128 increments). Each spectrum required 35 min.

Supernatant samples for NMR experiments comprised 90:10 (v:v) mixture of supernatant: D_2O in a standard 5 mm NMR tube. ^{1}H-^{15}N HMQC spectra were acquired as described above. Cell lysate samples for NMR experiments comprised 90:10 (v:v) mixture of cell lysate: D_2O in a standard 5 mm NMR tube. ^{1}H-^{15}N HMQC spectra were acquired as described above.

2.3 Results and Discussion

^{1}H-^{15}N SOFAST HMQC spectra of *E. coli* expressing the periplasmic protein HdeA were obtained 3 h after inducing with IPTG (Fig 2.5.1). Protein resonances were visible in the cell slurry (Fig 2.5.1A). To check for leakage, the slurry was centrifuged and a spectrum of the supernatant acquired. The spectrum of the slurry showed a strong protein signal (Fig 1B), similar to that observed in the lysate (Fig 1C). The observation of HdeA crosspeaks in the supernatant indicates leakage. The approximate periplasmic protein concentration after 3 h of expression is shown in Table 2.6.1.

To assess if expression levels contribute to leakage, the spectrum of the cell slurry that had been allowed to express HdeA for only 1.5 h was acquired (Fig 2.5.2). Crosspeaks characteristic of HdeA are not observed (Fig 2.5.2A,B) but metabolite signals are observed [36]. In comparison, the lysate contains resonances typical of

HdeA (Fig 2.5.2C). We then determined the amount of HdeA/cell after 1.5 h of expression (Table 2.6.1).

We also examined the protein CI2 (Fig. 2.5.3). After 1.5 h of expression, crosspeaks from CI2 are not visible in the cell slurry or cell supernatant (Fig 2.5.3A,C), but are visible in the lysate (Fig 2.5.3E). Spectra collected after 3 h of expression show leakage (Fig 2.5.3 B,D,F), in agreement with other results [27]. The amount of CI2/cell after 1.5 and 3 h of expression are given in Table 2.6.1.

We also examined the proteins α-synuclein and ubiquitin. Spectra like those collected in Figures 1 and 2 for these proteins show that they do not leak, in agreement with a previous study [27]. The amounts for these proteins per cell after 1.5 and 3 h of expression are given in Table 2.6.1.

We compared location and concentrations for four proteins in *E. coli* cells to the observation of leakage. Ubiquitin and HdeA are exclusively localized in the cytoplasm and periplasm respectively [30, 32]. CI2 and α-synuclein, however, have been shown to localize in both the periplasmic and cytoplasmic regions of the cell [11, 27]. For this reason, the amount of protein expressed per cell was determined and then used to calculate the intracellular concentrations. The results in Table 2.6.1 suggest that leakage is associated with high intracellular concentrations.

We showed that leaking begins if intracellular concentrations of approximately 7.5 ±0.7 mM are exceeded for proteins that are exclusively expressed in the periplasm. For a protein found throughout the cell like CI2, intracellular concentrations exceeding 20.2 ±0.9 mM results in leakage. In comparison, α-synuclein is found throughout the cell but has an intracellular concentration of only 4.0 ±1.1 mM after 3 h of expression. Thus,

leakage does not occur for proteins expressed at lower levels. Our conclusion is supported by previous results on CI2, which showed this protein does not leak when expressed using the less efficient trifluoromethyl-L-phenylalanine expression system [27].

Assuming that expression of other proteins is decreased to maintain the 400 g/L cellular concentration while our protein is overexpressed, we were able to determine the percentage of our protein's mass to the mass of total cellular protein. We calculated that 20-25% of the macromolecular mass in the cell is our protein before leaking begins. For the protein CI2, leaking is observed at the intracellular concentrations of 20.2 ±1.0 mM, which equates to approximately 37%.

Although highly expressed proteins leak, the mechanism is unknown. Li et al estimated that the total amount of CI2 found in the supernatant of the cell slurry is approximately 5-10% [27]. Previous in-cell NMR experiments performed in *E. coli* show that approximately 90-95% of the cells remain viable [37]. These data suggest that the CI2 found in the supernatant is the product of cell lysis. CI2, normally a cytoplasmic protein, is also found within the periplasmic space after overexpression [27]. This observation suggests that passive exocytosis may also contribute to protein leakage.

2.4 Conclusion

In summary, we have shown that overexpression can lead to leakage if the intracellular concentration of the protein exceeds ~10 mM. In-cell NMR experiments in *E. coli* should consider this expression limit so that valid data are obtained within the cell. For globular proteins, the leaked protein contributes to 100% of the ^{1}H -^{15}N NMR

spectrum because the intracellular environment broadens ^{1}H -^{15}N crosspeaks beyond detection [27]. Future in-cell NMR experiments in *E.coli* cells should consider intracellular concentrations low enough to obtain valid in-cell data.

2.5 Figures

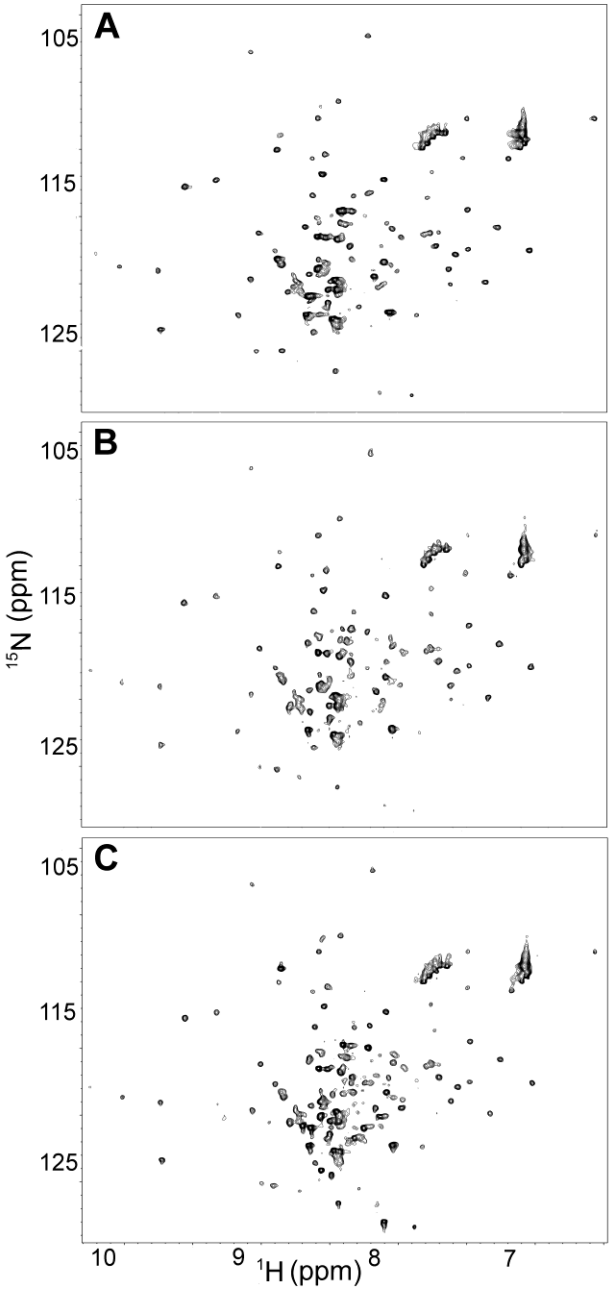

Figure 2.3.1. In-cell SOFAST ^{15}N – ^{1}H HMQC spectra (37°C) of *E. coli* expressing HdeA after 1.5 h.
Panel A: In-cell spectrum. Panel B: Spectrum of supernatant acquired immediately after acquisition of in-cell spectrum. Panel C: Spectrum of cell lysate.

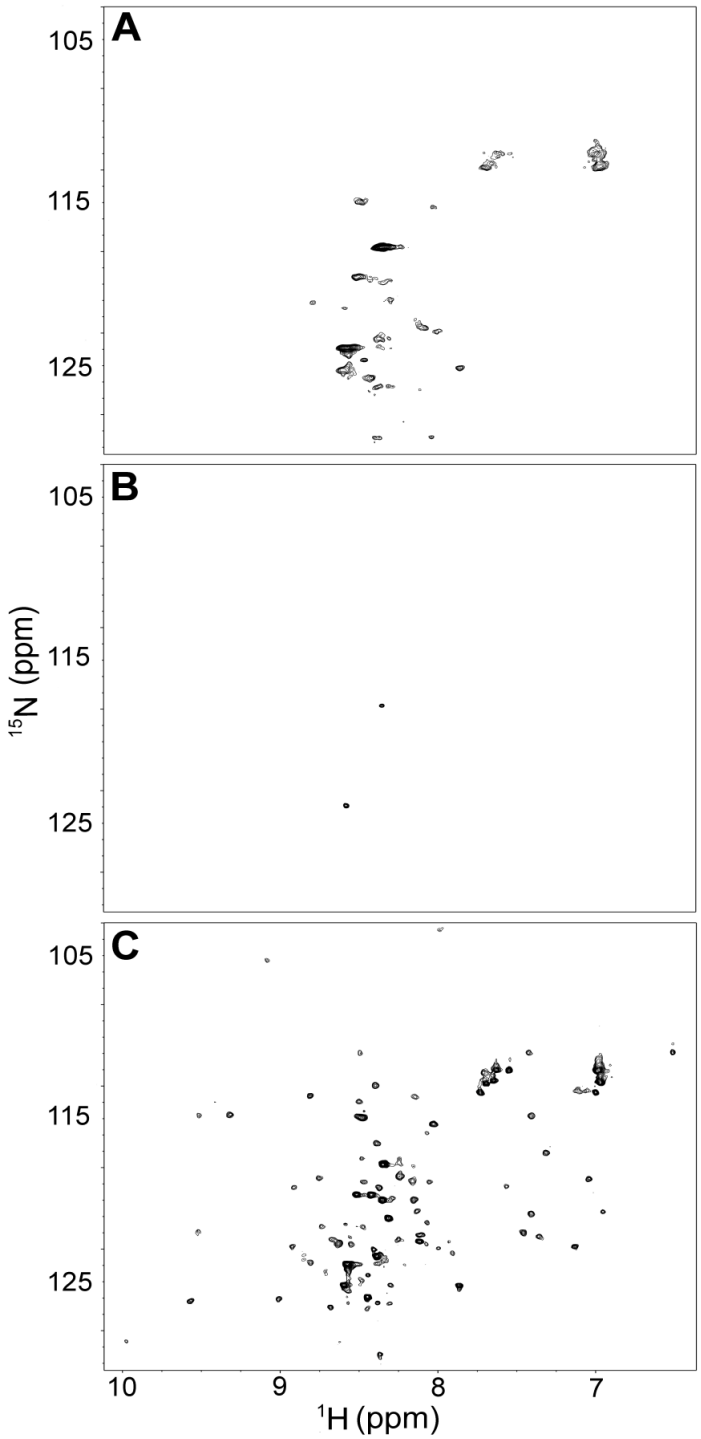

Figure 2.2.3. In-cell SOFAST ^{15}N – ^{1}H HMQC spectra (37°C) of *E. coli* expressing HdeA after 1.5 h.
The panels are described as in the legend to Figure 2.1.

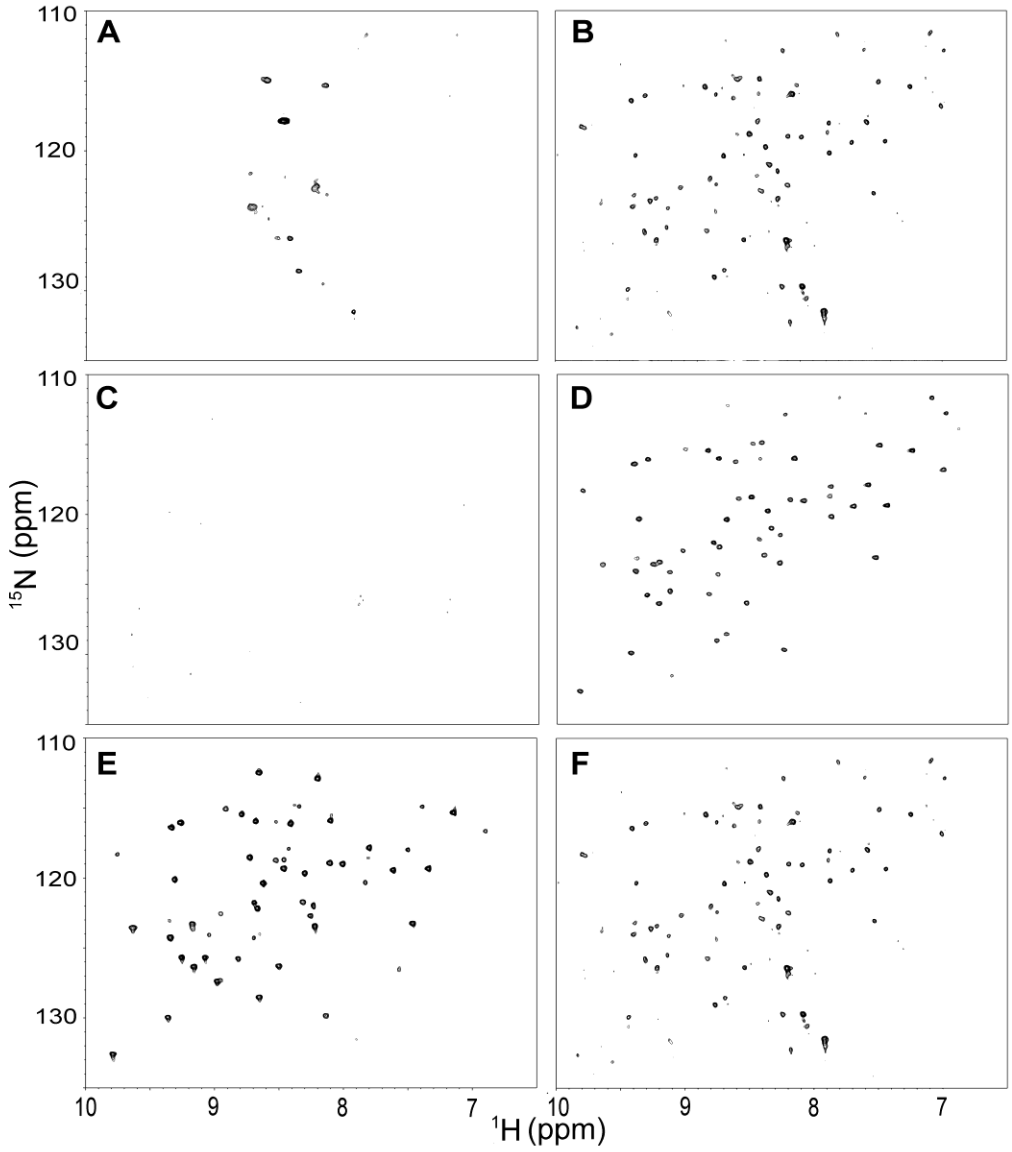

Figure 2.5.3. In-cell SOFAST ^{15}N – ^{1}H HMQC spectra (37°C) of *E. coli* expressing CI2 after 1.5 h (left panels) and 3 h (right panels).
Panels A-B: In-cell spectra. Panels C-D: Spectra of supernatant immediately after acquisition of in-cell spectra. Panels E-F: Spectra of cell lysate.

Table 2.6.1. Protein Intracellular Concentrations

Table I. Intracellular Concentrations[a]

Protein	Expression Level (fg/cell)		
	After 1.5 h	After 3 h	Location
HdeA	90 ± 10[b]	140 ±10	Periplasim
α-Synuclein	30 ± 10	60 ± 20[c]	Periplasm/Cytoplasm
Chymotrpysin Inhibitor 2	80 ±10	150 ±10	Cytoplasm/Periplasm
Ubiquitin	10 ± 5	40 ±10	Cytoplasm

[a]Quantified by integrating pixel intensities of bands from Coomassie-stained SDS PAGE and comparing them against standards of the pure proteins.
[b]Standard error, n=4. [c]Does Not Leak

3 A Bioreactor for in-cell protein NMR

3.1 Introduction

Most biophysical experiments on investigate proteins are conducted in dilute solution. Most proteins, however, serve their physiologically relevant function in cells, which have a complex crowded environment that affect several protein properties compared to dilute solution [38-41]. For this reason, there is an increasing interest in studying proteins inside living cells. Nuclear magnetic resonance spectroscopy (NMR) has become a popular tool for experiments on living cells because it provides atomic-level information about cellular components and is nondestructive [42].

A disadvantage of NMR spectroscopy is its low sensitivity. Selective isotopic enrichment or labeling of the targeted species with an NMR active nucleus (e.g., ^{15}N, ^{13}C or ^{19}F) is one way around this problem. Serber *et al.* suggest that the minimum concentration of the protein under study should be at least ~150 μM for ^{15}N enrichment or ~50 μM for ^{13}C enrichment [21]. Therefore, the target protein must be overexpressed or introduced into the cell by other means (e.g., micro injection, cell penetrating peptides [42]). To increase sensitivity further, high cell densities (10^9-10^{11} cells/mL) are used, and the data are time averaged.

Current experimental setups for protein in cell NMR have several drawbacks. First, the lack of aeration and the high cell density create an anaerobic environment. Second, metabolites and waste products accumulate. These characteristics can decrease cell viability, limiting the cell types that can be used, and make it difficult to

monitor temporal changes. Overcoming these challenges requires an NMR compatible device that maintains cell viability.

Devices with these characteristics have been developed. One type is an in-magnet bioreactor that enables growth of microorganisms to a high density [43, 44]. Another type is a perfusion system that flows media **down** through immobilized cells [45, 46]. These devices tend to be complex and difficult to fabricate. Furthermore, they are designed for studying metabolism.

Here, we describe a circulating encapsulated cells (CEC) bioreactor and accessories for in-cell protein NMR. The instrument comprises parts that are commercially available or easily fabricated. The expression of the natively disordered human protein α-synuclein in *Escherichia coli i*s used to demonstrate its capabilities. α-Synuclein is a 14.5 kDa protein implicated in the pathogenesis of Parkinson's disease [47]. The expression of the plasmid borne α-synuclein gene is controlled by a lactose inducible, phage T7 promoter. We investigate the bioreactor's ability to maintain cell viability and measure the accumulation of α-synuclein with time.

3.2 Materials and Methods

3.2.1 Purification of wild type α-synuclein for in vitro experiments

The pT7-7 plasmid containing the α-synuclein gene was transformed into *E. coli* Bl-21 (DE3) Gold cells (Strategene). Plasmid containing cells were selected with 0.1 mg/mL ampicillin. A 5 mL overnight culture was grown from a single colony and used to inoculate a 50 mL culture of Spectra 9 ^{15}N-enriched media (Cambridge Isotope

Laboratories) at 37°C in a rotary shaker (225 rpm, New Burnswick Scientific, Model I-26). The saturated overnight culture was used to inoculate 1 L of M9 minimal media [48] containing 1 g/L $^{15}NH_4Cl$. After reaching an absorbance at 600 nm (A_{600}) of 0.8-1.0, the culture was induced with isopropyl β-D-thiogalactopyranoside (IPTG) to a final concentration of 1 mM. The culture was placed in the rotary shaker (225 rpm) at 37°C.

After 5 h the cultures were pelleted using a swinging bucket centrifuge (Sorvall RC-3B, H6000A rotor) at 1600*g* for 30 min at 4°C and the pellet was stored at -20°C. The pellet was resuspended in 30 mL of lysis buffer (50 mM Tris, 150 mM NaCl, 1 mM phenylmethanesulfonyl fluoride, 0.4 g/L lysozyme, pH 8.0). RNase and DNase were added to a final concentration of 0.02 g/L each. The samples were stirred (250 rpm) at 4°C for 20 min. The lysate was sonicated (Branson Ultrasonics, Fischer Scientific) continuously for 5 min, boiled in a water bath for 20 min, and then centrifuged at 13,000*g* for 30 min at 4°C (SS-34 rotor). The supernatant was subjected to streptomycin sulfate precipitation (10 g/L) and centrifuged for 30 min at 4°C. The supernatant was subjected to $(NH_4)_2SO_4$ precipitation (361 g/L) and centrifuged again for 30 min at 4°C. The pellet was resuspended in 20 mM sodium phosphate buffer (pH 7.4) and dialyzed (Thermo Scientific, 3500 MWCO) overnight, with stirring at 4°C, against the same buffer.

The protein was further purified by anion exchange chromatography (GEHealtcare, Q Sepharose HiPrep 16/10 column) with a 0-1 M linear gradient of NaCl in 20 mM phosphate buffer (pH 7.4). Fractions were subjected to SDS-PAGE on an 18% gel with Commassie blilliant blue staining. Fractions containing α-synuclein were pooled and dialyzed against water overnight, with stirring, at 4°C. The protein was

concentrated in a YM-3 Centricon filter (Millipore, MWCO 3500) using centrifugation at 1000*g* (SS-34 rotor) for 1 h at 4°C. The purity of the protein was determined by SDS-PAGE with Coomassie staining. The pure α-synuclein was lyophilized (Labconco) and stored at -20°C. The yield was 35-60 mg of pure α-synuclein per liter of saturated cell culture.

3.2.2 Cultivation of *E. coli* for in-cell NMR experiments

A 5 mL overnight culture was grown from a single colony and used to inoculate a 500-mL Erlenmeyer flask containing 50 mL of isotopically enriched media, as described above. After the culture reached an A_{600} of 0.8-1.0, the cells were induced with IPTG to a final concentration of 1 mM. Expression was allowed to proceed for 4 h. The cells were gently harvested by using the swinging bucket centrifuge for 30 min at 4°C. The pellet was resuspended in 1 mL of spent media.

3.2.3 Cultivation and encapsulation of *E. coli* for NMR bioreactor experiments

A 5 mL overnight culture was grown from a single colony as described above and used to inoculate 150 mL of Luria Broth (10 mg/mL Tryptone, 5 mg/mL yeast extract, 10 mg/mL NaCl) at 37°C. The culture was grown in the rotary shaker (225 rpm) to an A_{600} of 0.8-1.0. The cells were gently harvested in the swinging bucket centrifuge for 20 min at 4°C and resuspended in 1 mL of spent media. The resuspended cells were mixed with a 2% w/v alginate (Sigma) solution in 20 mM phosphate, 150 mM NaCl (pH 7.4) to give a final concentration of 1% alginate (50:50 mixture alginate:cell slurry).

The electrostatic encapsulation device (Fig. 3.5.7) comprised a 1 mL insulin syringe (BD), a 24 gauge winged anigocatheter (0.7 x 19 mm tip, Braun), a 23 gauge needle (BD), a syringe pump (Braintree Scientific 8000), and an adjustable high voltage power supply (Spellman SL10). The insulin syringe, equipped with the needle, was loaded with the cell/alginate mixture. The other needle, which was inserted horizontally through the center of the angiocatheter, was connected to the positive pole of the power supply. The negative pole of the power supply was placed into the 150 mM $CaCl_2$ solution. The syringe containing the mixture was inserted into the top of the angiocatheter and placed onto the pump. The syringe pump was set to a rate of 0.714 mL/min, the power supply voltage to 3.35 kV, and the stir-plate to approximately 300 rpm. The tip of the angiocatheter was centered 1.2 cm above a 250 mL beaker containing 150 mL of 150 mM $CaCl_2$. The mixture was forced through the tip of the angiocatheter and streamed into the $CaCl_2$ solution. The Ca^{2+} polymerizes the alginate which, in turn, forms encapsulated beads containing the cells. The encapsulated cells were retrieved with suction and placed in a 15 mL Falcon tube containing 150 mM $CaCl_2$ solution for transport to the NMR spectrometer.

The $CaCl_2$ solution was removed and the encapsulated cells were washed with the phosphate-free minimal medium. The phosphate-free minimal medium consisted of 100 mM HEPES (pH 7.4), 150 mM $CaCl_2$, phosphate-free M9 salts [1mg/mL $^{15}NH_4Cl$, 2 mM $MgCl_2$, 1 µg/mL thiamine, 2 % v:v 10x ^{15}N-enriched Bioexpress 1000 media (Cambridge Isotope Laboratories)] and 0.1 mg/mL ampicillin. After washing, the encapsulated cells were placed inside the bioreactor, which was then placed into the spectrometer. After acquiring the initial spectrum, lactose was added to a final

concentration of 1% w/v. The lactose acts as an inducer and the sole carbon source. For each spectrum, the pump circulated medium through the system at a rate of 45 mL/min for 30 min. Five min were allotted for the encapsulated cells to settle into the detection region of the bioreactor. As a control the procedure was repeated for *E. coli* containing the pUC18 plasmid.

3.2.4 NMR

Data were acquired at the UNC Biomeolcular NMR facility on a Varian Inova 600 MHz NMR spectrometer. Data were processed and visualized with NMRpipe and NMRviewJ, respectively [34, 35].

Samples for dilute solution spectra comprised a 90:10 (v:v, pH 7.4) mixture of purified 200 μM α-synuclein solution: D_2O in a standard 5 mm NMR tube. ^{1}H-^{15}N HSQC spectra were acquired at 10^{o}C [1] with a 5 mm Varian Triax triple resonance probe (^{1}H sweep width: 11990.40 Hz; ^{15}N sweep width: 2100 Hz, 8 transients, 128 increments). Each spectrum required 35 min.

Samples for simple in-cell NMR experiments comprised 90:10 (v:v) mixture of resuspended cells: D_2O in a standard 5 mm NMR tube. ^{1}H-^{15}N HSQC [49, 50] spectra were acquired as described above, except with 12 transients and 128 increments. Each spectrum required 1 h.

Samples for encapsulated in-cell NMR experiments comprised encapsulates in a 90:10 (v:v) mixture of 150 mM $CaCl_2$: D_2O in a standard 5 mm NMR tube. For encapsulates in standard 5 mm NMR tubes, ^{1}H-^{15}N HSQC spectra were acquired as described above. In the bioreactor, ^{1}H-^{15}N HSQC spectra were acquired unlocked at

37^{o}C with an 8 mm modified Varian Triax triple resonance z gradient probe as described above. Samples for NMR bioreactor experiments comprised encapsulated cells in phosphate-free media supplemented with Bioexpress 1000. ^{1}H-^{15}N SOFAST HMQC spectra were acquired unlocked at 37^{o}C as described above, except with 48 transients and 96 increments. Each spectrum required 35 min.

3.3 Results

3.3.1 The CEC bioreactor

The bioreactor is made from Teflon to facilitate NMR experiments involving ^{1}H detection (We have made a similar version from Plexiglass for ^{19}F detection). It consists of three main parts; an 8 mm diameter tube, a circulation chamber, and an adjustable threaded cap (Fig. 3.5.1). An inlet for an Upchurch Scientific Super Flangeless Fitting is located on the upper part of the cap (Fig. 3.5.1E). A 1/16" OD inlet for Upchurch Scientific perfluoro alkoxy alkane tubing is located at the bottom (Fig. 3.5.1A).

Most of the components (Fig. 3.5.2) are commercially available. The liquid media is contained in a 1 L Corning three neck spinner flask with a tubing adaptor on one side arm (Fig. 3.5.2A). A peristaltic MasterFlex pump (Fig. 3.5.2B), moves the media at a rate of 45 ml/min from the flask, through the tubing adaptor, into the PFA tubing (Fig. 3.5.2, yellow lines). The tubing runs from the pump, into the bottom of an 8 mm Varian triple resonance z gradient probe through an opening created by removing the heater (Fig. 3.5.2D). The temperature is controlled with the spectrometer's FTS Systems heating apparatus (Model TC-84). PFA tubing between the pump and the

bioreactor is placed in a Fisher Scientific Isotemp water bath to warm the media (Fig. 3.5.2C), which flows from the bottom of the bioreactor to the top (Fig. 3.5.1, arrows on right side). The PFA tubing at the top of the bioreactor returns the media, via a pH probe, to the 1 L the Corning three neck spinner flask. The pH probe, pump and NMR spectrometer are connected to a laptop computer (Fig. 3.5.2, green lines).

The ^{1}H-^{15}N band-selective optimized flip-angle short transient (SOFAST) heteronuclear multiple quantum coherence (HMQC) [51] pulse program provided in the Varian Biopak suite of pulse sequences was modified to send voltage outputs to the computer. The signals are interpreted by LabView (National Instruments) software, which controls the pump. The software also records the pH value at 1 min intervals.

Cells are electrostatically encapsulated into 1 mm diameter Ca^{2+} alginate spheres to keep them in the bioreactor [52]. The circulation of the encapsulated cells facilitates the delivery of nutrients and waste removal. The bioreactor (Fig. 3.5.1) has two states: pump off, and pump on. When the pump is off, encapsulated cells settle into the 8 mm diameter tube for data acquisition (Fig. 3.5.1, left panel). When the pump is on, the encapsulates travel from the 8 mm diameter tube into the wider circulation chamber. The movement of the encapsulates from a narrow to wider tube results in a reduction in pressure causing the encapsulates to circulate in the chamber (Fig. 3.5.1, right panel). The pulsed, upward motion also prevents the encapsulates from clogging the outlet of the cell chamber.

3.3.2 CEC bioreactor without flowing media

To assess the bioreactor's suitability for in cell NMR experiments, the ^{1}H-^{15}N HSQC spectrum of encapsulated *E. coli* in the bioreactor is compared to the HSQC spectrucm of ^{15}N enriched α-synuclein obtained in a conventional 5 mm NMR probe (Fig. 3.5.3A,B). The in vitro spectrum of purified α-synuclein (Fig. 3.5.3C) is shown as a reference. The similarity of the spectra indicates that α-synuclein can be detected in the bioreactor.

To assess the bioreactor's effect on spectral quality, the in cell HSQC spectrum of encapsulated *E. coli* expressing ^{15}N enriched α-synuclein in the bioreactor is compared to the HSQC spectrum of the same encapsulates in a 5 mm tube (Fig. 3.5.3A,D). The spectrum of the encapsulated cells in the 5 mm tube is consistent with the published spectrum [53]. The crosspeaks broaden when encapsulates are placed in the bioreactor, but the quality of spectra is only slightly degraded.

3.3.3 CEC bioreactor with flowing media

The expression of α-synuclein was monitored with the ^{1}H-^{15}N SOFAST HMQC pulse sequence, rather than the HSQC sequence, to obtain higher sensitivity and decrease acquisitions times. Spectra as a function of time are shown in Fig. 3.5.4A-C. The spectrum of the encapsulates before induction (Fig. 4A) has few crosspeaks and no unambiguous α-synuclein crosspeaks. After induction new crosspeaks begin to appear. With each successive spectrum, the crosspeaks increase in volume as seen at 4 h and 18 h (Figs. 3.5.4B,C). Using methods described by Slade et al. [54] we determined the intracellular concentration of α-synuclein to be 0.8 mM at 18 h.

As a control, the encapsulates were removed after the experiment and a spectrum was acquired of the surrounding media (Fig. 3.5.4D). The spectrum shows only a weak crosspeak, indicating that the bulk of the signal comes from the encapsulated cells. The viability of the *E. coli* in the bioreactor experiments was determined by plating serial dilutions of dissolved encapsulates before and after each experiment. The viability was 95%. The pH of the medium perfused around the encapsulated cells remained at 7.00 for the duration of the experiment.

Although the CEC bioreactor provides an environment where encapsulated *E. coli* cells express α-synuclein, the lower resolution of SOFAST HMQC spectra can make it difficult to distinguish between metabolites and protein crosspeaks. To determine which crosspeaks corresponded to α-synuclein, we collected spectra of fresh media (Fig 3.5.5A) and of *E. coli* containing a pUC18 plasmid [55] without the α-synuclein gene (Fig 3.5.5B). Overlaying these spectra with the spectrum of α-synuclein expressed in the bioreactor (Fig 3.5.5C), shows that most of the crosspeaks are from α-synuclein (Fig 3.5.5D).

The overlay allowed us to quantify temporal changes in crosspeak volumes (Fig 3.5.6). The crosspeak from the defined minimal media is the only crosspeak detectable at 30 min (Fig 3.5.6H). Although induction occurred at 30 min, there was a lag phase of approximately 4 h before crosspeaks could be detected (Fig 3.5.6A-B, E-G). Some crosspeaks are not detectable until approximately 7 h (Fig 3.5.6C,D),

The volumes of α-synuclein crosspeaks increased with time, beginning with a lag phase before growing exponentially to a plateau (Fig 3.5.6A-E). One crosspeak deviated from this trend (Fig 3.5.6D), most likely because the poor resolution in this

area of the spectrum (Fig 3.5.5D). Temporal changes in crosspeak volumes for two metabolites showed different trends. One metabolite remained constant (Fig 3.5.6F), while the other metabolite showed a time dependence that resembled the α-synuclein crosspeaks (Fig 3.5.6G). The crosspeak from the defined minimal media, is the only crosspeak that showed a slight decrease in intensity with time (Fig 3.5.6H).

3.4 Discussion

The CEC bioreactor (Fig. 3.5.1) is designed to provide a controlled environment for NMR experiments involving living cells. It allows media to deliver nutrients and remove waste from encapsulated cells contained in a circulation chamber (Fig. 3.5.1, right panel). When the flow of media is stopped, the encapsulated cells settle allowing data acquisition (Fig. 3.5.1, left panel).

In the experimental setup, the CEC bioreactor is the only component located inside the spectrometer (Fig. 3.5.2). This configuration allows the external components to be altered without removing the bioreactor before or during the experiment, facilitating studies requiring different conditions in one experiment. The setup is also versatile. Different solution probes and sensors can be inserted between the external components. The tubing can be rerouted, for example, to send the media to a waste container. In addition, the material used to make the bioreactor can be changed for experiments requiring different isotopic nuclei detection. Here we use Teflon for ^{15}N detection, but a Plexiglass bioreactor can be used for ^{19}F NMR.

To our knowledge, the CEC bioreactor is the first bioreactor suitable for protein in cell NMR experiments (Fig. 3.5.3A,B). The design provides an environment where

encapsulated cells can express protein while maintaining reasonably high quality in cell NMR spectra (Fig 3.5.3C-D). Furthermore, the bioreactor can be used to quantify temporal changes in crosspeak volumes during the experiment (Fig. 3.5.4 and 5).

Our data allow us to draw several conclusions. We showed that α-synuclein was present at an intracellular concentration of 0.8 mM at 18 h. Using information from Figure 6, we conclude that the detection limit for in-cell NMR is approximately 0.14 mM. This finding is consistent with other work on the minimal intracellular protein concentration needed for in-cell NMR [6]. For most residues, the detection limit is achieved after 3 h. Two protein crosspeaks do not follow this trend in that they are not detectable until approximately 7 h (Fig. 3.5.6 C,D). The crosspeaks from glycine residues that comprise the ear shaped pattern in the upper left region of α-synuclein Figure 3.5.4 (^{15}N ppm 108-113, ^{1}H ppm 8.3-8.7), follow a similar trend. The delay in detectability may be due to differential binding of α-synuclein to other intracellular components, which broadens their crosspeaks. Another possibility for the delay is differential relaxation, because *in vitro* models for α-synuclein dynamics show that certain residues experience less mobility [17]. Decreased mobility produces broader, weaker signals, which would explain the longer time required to detect them.

3.5 Conclusion

In summary, the CEC bioreactor provides a controlled environment where protein NMR spectra data can be acquired in living *E. coli* cells. Our next goal is to show that the CEC bioreactor is compatible with other cell types, and is versatile enough for metabolomic, as well as protein NMR experiments. We specifically want to focus on

eukaryotic cells whose viability is adversly affected by current methods. Progress has been made in maintaining the viability of CHO cells using our device for 48 h, but other cell lines have yet to be tested. Our long-term goal is to monitor temporal changes in protein structure and metabolism due to perturbations, such as drug interactions, in human cells, and so increase the understanding of intracellular components under physiological conditions.

3.6 Figures

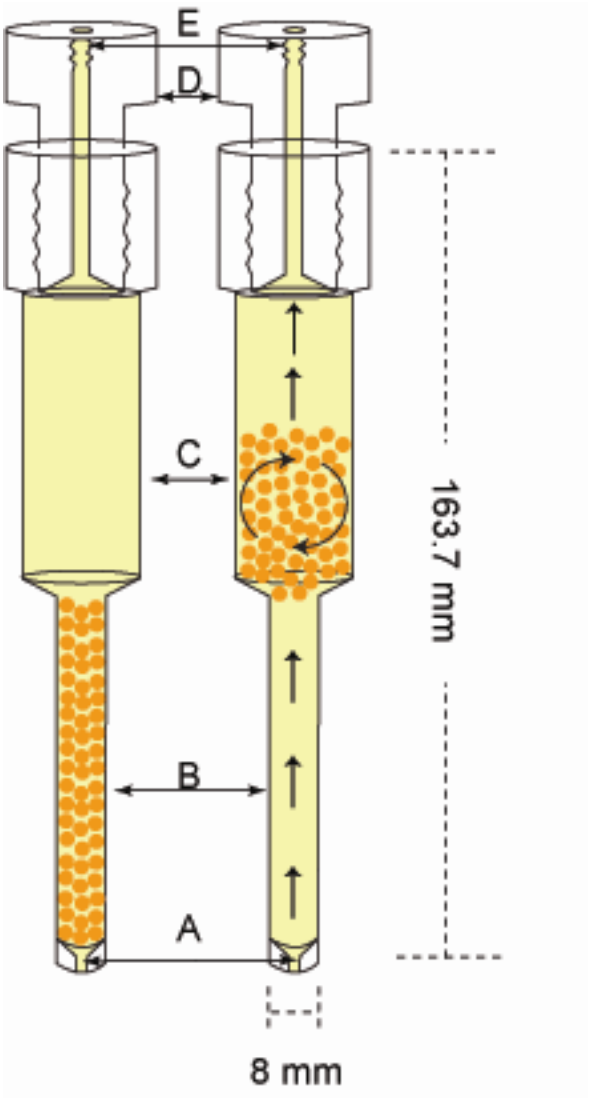

Figure 3.6.1. The CEC bioreactor.
On the left, the pump is off and the encapsulates are settled. On the right, the pump is on and the encapsulates circulate at a steady state in the upper chamber. A: tubing inlet, B: NMR detection region, C: circulation chamber, D: adjustable threaded cap, E: fitting inlet. Orange circles represent encapsulates containing *E. coli* cells.

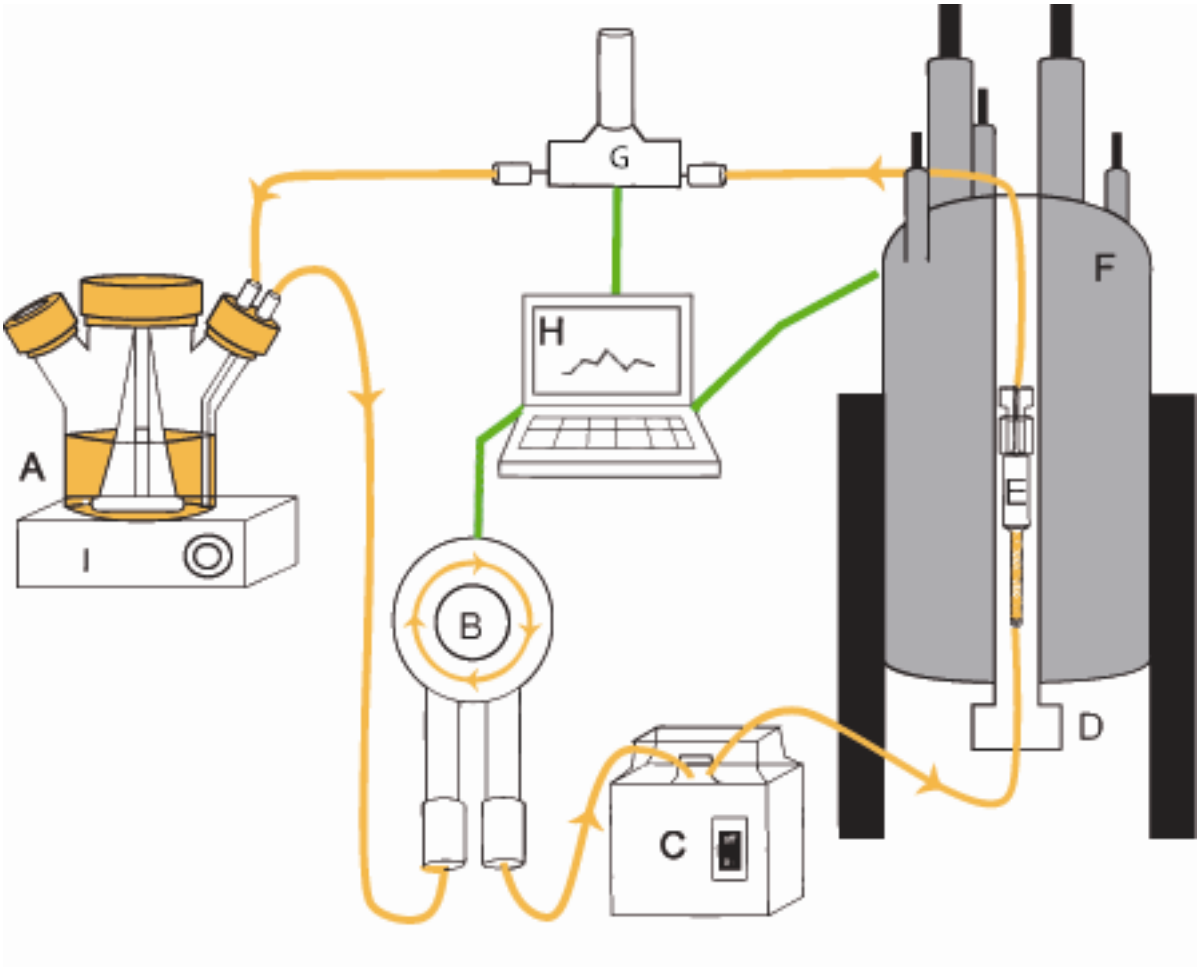

Figure 3.6.2. The experimental set-up.
A: Corning spinner flask fitted with a vented cap on one side arm and tubing adaptors on the other, B: peristaltic pump, C: water bath, D: 8 mm probe with heater removed, E: bioreactor, F: magnet, G: pH probe, H: computer, I: stir plate.

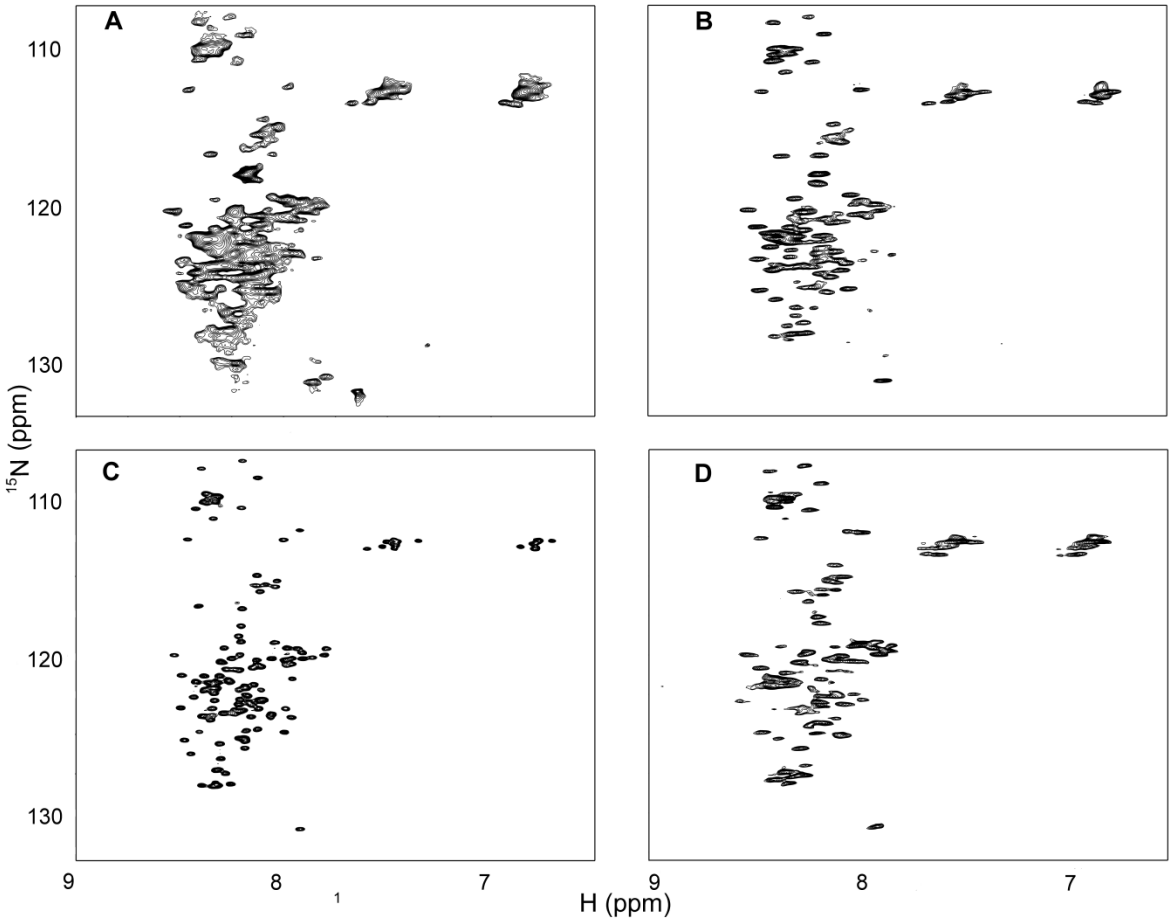

Figure 3.6.3. Comparing α-synuclein spectra.
Panel A: In cell HSQC spectrum of alginate encapsulated *E. coli* expressing α-synuclein in the bioreactor. Panel B: In cell HSQC spectrum of *E. coli* expressing α-synuclein. Panel C: *In vitro* HSQC spectrum of 200 μM purified wild type α-synuclein in HEPES buffer, pH 7.2 at 10°C. Panel D: In cell HSQC spectrum of alginate encapsulated *E. coli* expressing α-synuclein. The spectra shown in panels A, B & D were acquired at 37°C. The spectra in panels B-D were acquired in a 5 mm NMR tube using a 5 mm probe. The spectrum in panel A was acquired in the 8 mm bioreactor using an 8 mm probe.

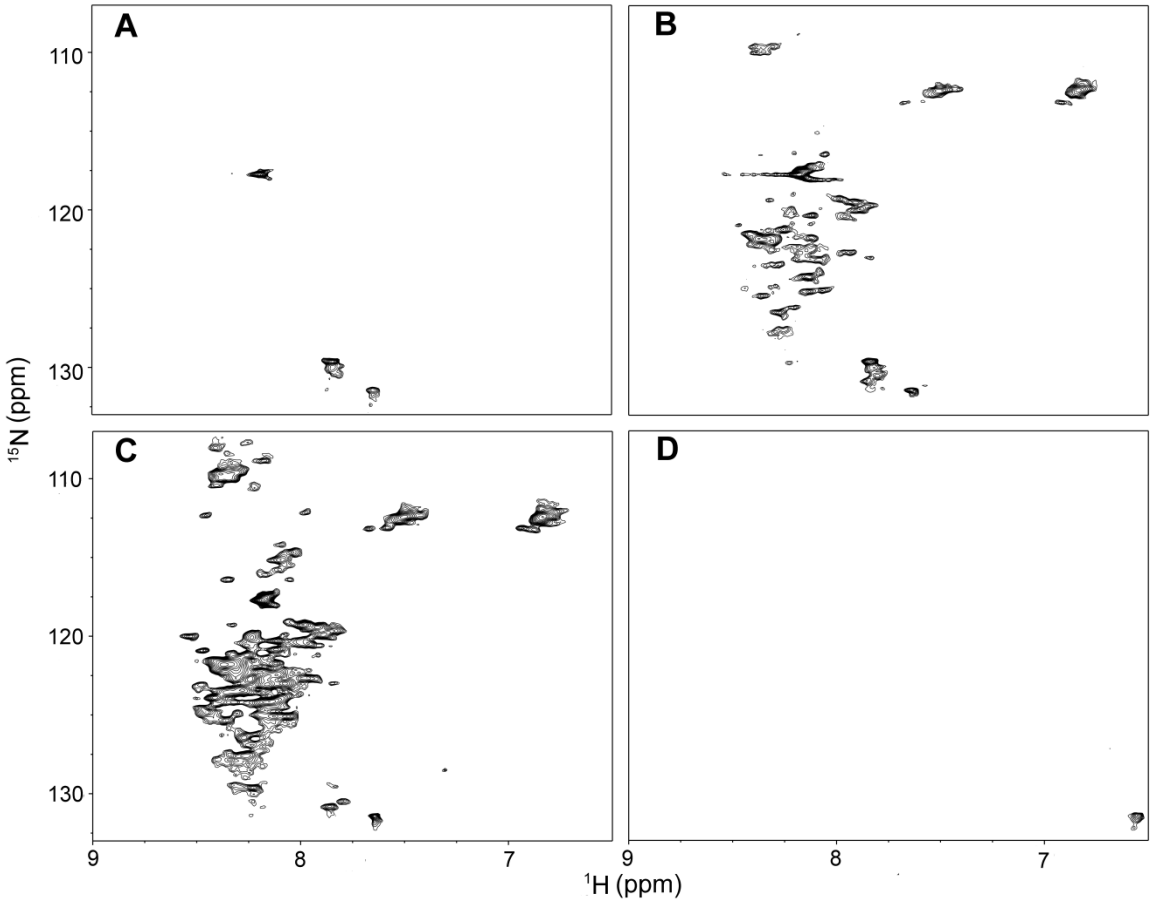

Figure 3.6.4. In-cell SOFAST ^{15}N-^{1}H HMQC [12] spectra (37°C) of *E. coli* expressing α-synuclein in the bioreactor.

Panel A: Spectrum collected before induction. Panel B: 4 h post induction. Panel C: 18 h post induction. Panel D: Spectrum of the spent medium.

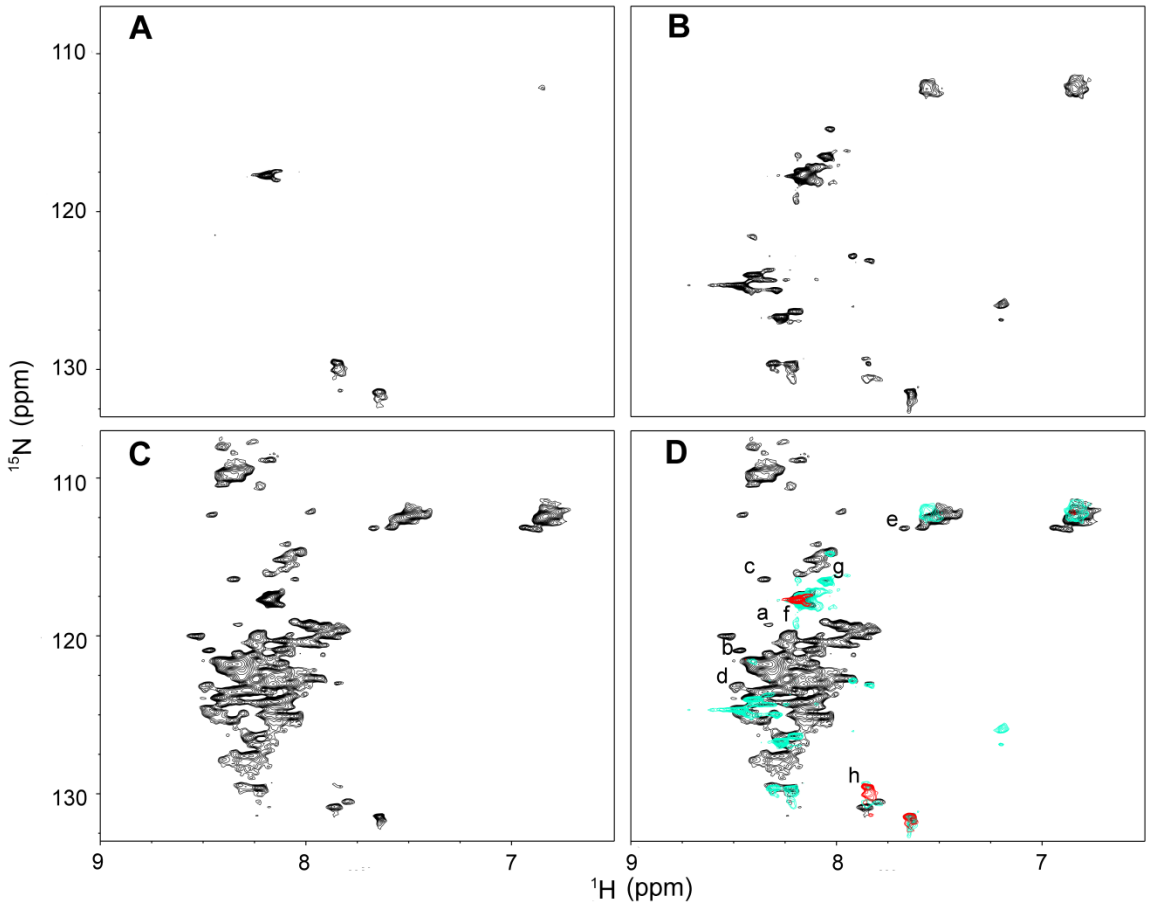

Figure 3.6.5. Determining which crosspeaks correspond to α-synuclein.
Panel A: In-cell SOFAST ^{15}N-^{1}H HMQC spectrum of the defined phosphate-free minimal media. Panel B: Spectrum of ^{15}N encriched encapsulated *E. coli* cells containing the control pUC18 plasmid. Panel C: Spectrum of encapsulated *E. coli* expressing α-synuclein. Panel D: Overlay of the spectra [medium (red), puc18 control cells (cyan), and α-synuclein (black)]. Crosspeaks used in subsequent analysis are labeled a-h. Spectra were acquired in the 8 mm bioreactor using an 8 mm probe at 37°C.

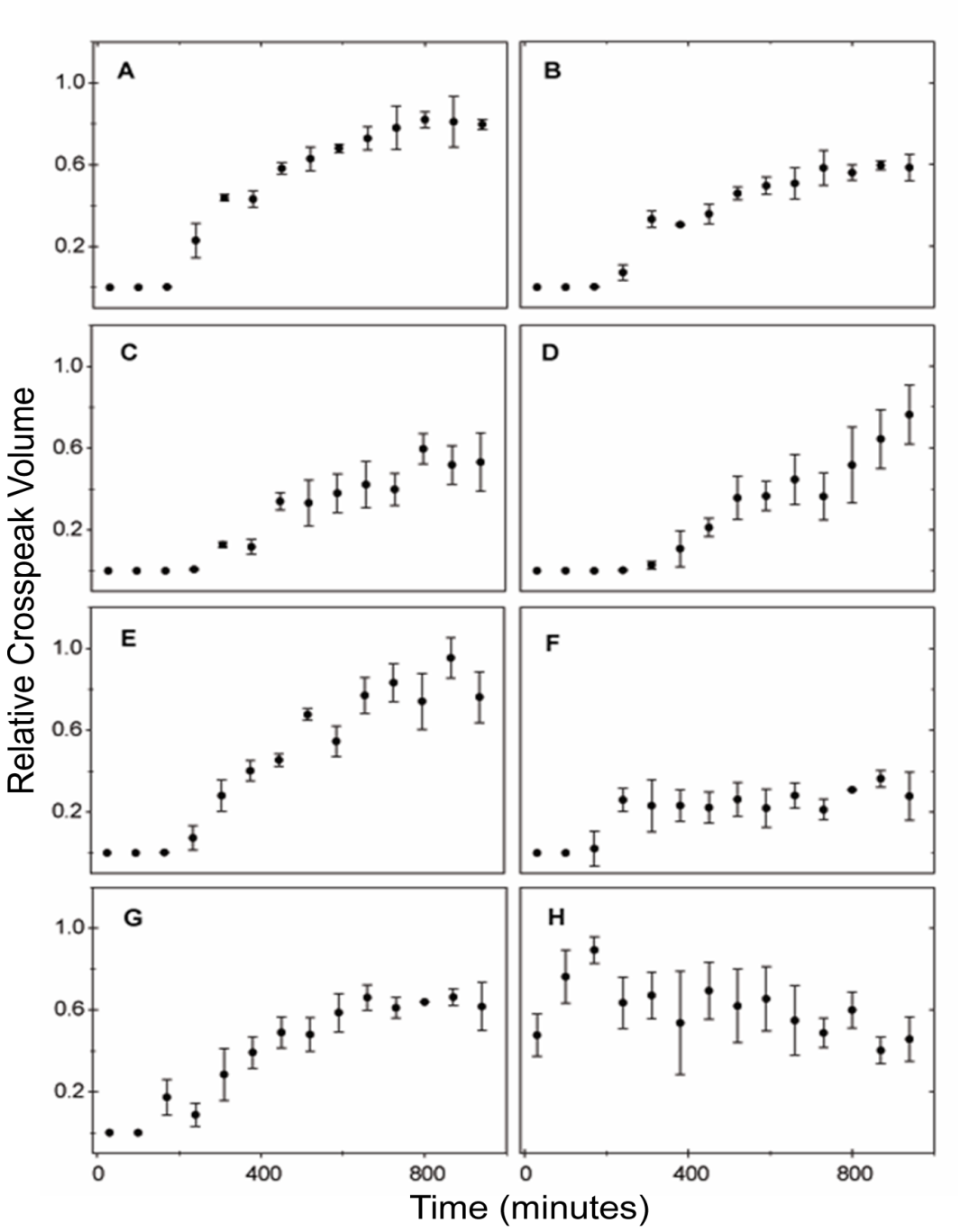

Figure 3.6.6. Temporal changes in crosspeak volume after inducing α-synuclein expression in the bioreactor.

Panels A-E: α-Synuclein crosspeaks. Panel F-G: Metabolite crosspeaks. Panel H: Crosspeaks from the defined phosphate free minimal media. Crosspeak volumes are normalized to the largest volume and are labeled in Figure 5D. Error bars represent the standard error from three independent experiments.

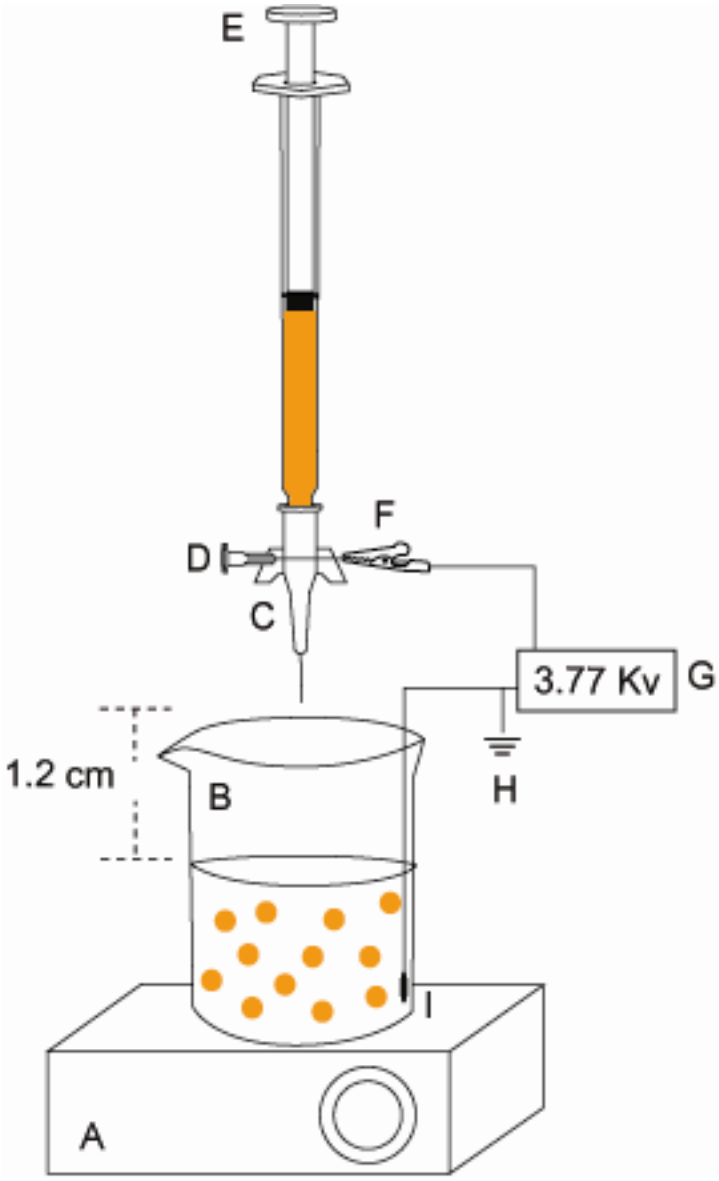

Figure 3.6.7. Schematic of the electrostatic encapsulation device.
A: stir plate, B: beaker containing 150 mM $CaCl_2$, C: anigocatheter, D: needle, E: insulin syringe, F: alligator clip (connects the positive power supply terminal to the needle) G: high voltage power supply, H: ground, I: negative end.

References

1. Cayley, D.S., Guttman, H. J., and Record, M.T., Jr., *Biophysical characterization of changes in amounts and activity of Escherichia coli cell and compartment water and turgor pressure in response to osmotic stress.* Biophys. J., 2000. **78**: p. 1748-1764.

2. Luby-Phelps, K., *Cytoarchitecture and physical properties of cytoplasm: Volume, viscosity, diffusion, intracellular surface area.* Int. Rev. Cytol, 2000. **192**: p. 189-221.

3. Laurent, T.C., *An early look at macromolecular crowding.* Biophys. Chem., 1995. **57**: p. 7-14.

4. Rohwer, J.M., Postma, P.W., Kholodenko, B.N., and Westerhoff, H.V., *Implications of macromolecular crowding for signal transduction and metabolite channeling.* Proc. Natl. Acad. Sci U.S.A., 1998. **95**: p. 10547-10552.

5. Phillip, Y., Sherman, E., Haran, G., and Schreiber, G., *Common crowding agents have only a small effect on protein-protein interactions.* Biophys. J., 2009. **97**(3): p. 875-885.

6. Acerenza, L., and Grana, M., *On the origins of a crowded cytoplasm.* J. Mol. Evol., 2006. **63**: p. 583-590.

7. Elowitz, M.B., Surette, M.G., Wolf, P.E., Stock, J.B., and Leibler, S., *Protein mobility in the cytoplasm of Escherichia coli.* J. Bacteriol., 1999. **181**: p. 197-203.

8. Lavalette, D., Hink, M.A., Tourbez, M., Tetreau, C., and Visser, A.J., *Proteins as micro viscosimeters: Brownian motion revisted.* Eur. Biophys. J., 2006. **35**: p. 517-522.

9. Li, C., Wang, Y., and Pielak, G.J., *Translational and rotational diffusion of a small globular protein under crowded conditions.* J. Phys. Chem., 2009. **113**: p. 13390-13392.

10. Mullineaux, C.W., Nenninger, A., Ray, N., and Robinson, C., *Diffusion of green fluorescent protein in three cell environments in Escherichia coli.* J. Bacteriol., 2006. **188**: p. 3442-3448.

11. Slade, K.M., Baker, R., Chua, M., Thompson, N.L., & Pielak, G.J., *Effects of Recombinant Protein Expression on Green Fluorescent Protein Diffusion in Escherichia coli.* Biochemistry, 2009. **48**: p. 5083-5089.

12. Dyson, J.H., and Wright, P.E., *Insights into the structure and dynamics of unfolded proteins fom nuclear magnetic resonance.* Adv. Protein Chem, 2002: p. 311-340.

13. Minton, A.P., *Models for excluded volume interaction between an unfolded protein and rigid macromolecular cosolutes: Macromolecular crowding and protein stability revisted.* Biophys. J., 2005. **88**: p. 971-985.

14. Charlton, L.M., Barnes, C.O., Li, C., Orans, J., Young, G.B., & Pielak, G.J., *Residue-level interrogation of macromolecular crowding effects on protein stability.* J. Am. Chem. Soc., 2008. **130**: p. 6826-6830.

15. Miklos, A.C., Li, C., and Pielak, G.J., *Using NMR-detected backbone amide ^{1}H exchange to assess macromolecular crowding effects on globular-protein stability.* Methods in Enzymology, 2009. **466**: p. 1-18.

16. Zhou, H.X., Rivas, G.N., and Minton, A.P., *Macromolecular crowding and confinement: Biochemical, biophysical, and potential physiological consequences.* Annu. Rev. Biophys., 2008. **37**: p. 375-397.

17. Ai, X., Zhou, Z., Bai, Y., & Choy, W.Y., *^{15}N NMR spin relaxation dispersion study of the molecular crowding effects on protein folding under native condtions.* J. Am. Chem. Soc., 2006. **138**: p. 3916-3917.

18. Homouz, D., Perham, M., Samiotakis, A., Cheung, M.S., & Wittung-Stafshede, *Crowded cell-like environment induces shape changes in aspherical protein.* Proc. Natl. Acad. Sci U.S.A., 2008. **105**: p. 11754-11759.

19. Brindle, K.M., Williams, S.P., and Boulton, M., *^{19}F NMR detection of a fluorine-labelled enzyme in vivo.* FEBS Lett, 1989. **255**: p. 121-124.

20. Serber, Z., Ledwidge, R., Miller, S.M., & Dötsch, V., *Evaluation of parameters critical to observing proteins inside living Escherichia coli by in-cell NMR spectroscopy.* J. Am. Chem. Soc., 2001. **123**: p. 8895-8901.

21. Serber, Z., et al., *Methyl groups as probes for proteins and complexes in in-cell NMR experiments.* Journal of the American Chemical Society, 2004. **126**(22): p. 7119-7125.

22. Dedmon, M.M., Patel, C.N., Young, G.B., and Pielak, G.J., *FlgM gains structure in living cells.* Proc. Natl. Acad. Sci. U.S.A., 2002. **99**: p. 12681-12684.

23. McNulty, B.C., Tripathy, A., Young, G.B., Charlton, L.C., Orans, J., & Pielak, G.J., *Temperature-induced reversible conformational change in the first 100 residues of alpha-synuclein.* Protein Sci, 2006. **15**: p. 602-608.

24. Pielak, G.J., Li, C., Miklos, A.C., Schlesinger, A.P., Slade, K.M., Wang, G., & Zigoneanu, I.G., *Protein Nuclear Magnetic Resonance under Physiological Conditions.* Biochemistry, 2009. **28**: p. 226-234.

25. Inomata, K., Ohno, A., Tochio, H., Isogai, S., Tenno, T., Nakase, I., Takeuchi, T., Futaki, S., Ito, Y., Hiroaki, H., & Shirakawa, M. , *High-resolution Multi-dimensional NMR Spectroscopy of Proteins in Human Cells.* Nature, 2009. **458**: p. 106-109.

26. Selenko, P., & Wagner, G., *Looking into live cells with in-cell NMR spectroscopy.* J. Struct. Bio., 2007. **158**(2): p. 244-253.

27. Li, C., Wang, Wang, Y., Creager-Allen, R., Lutz, E.A., Scronce, H., Slade, K.M., Ruf, R.A.S., Mehl, R.A., & Pielak, G.J., *Protein ^{19}F NMR in Escherichia coli.* J. Am. Chem. Soc., 2009. **132**: p. 321-327.

28. Li, C., Charlton, L.M., Lakkavaram, A., Seagle, C., Wang, G., Young, G.B., MacDonald, J.M., & Pielak, G.J., *Differential dynamical effects of macromolecular crowding on an intrinsically disordered protein and a globular protein: implications for in-cell NMR spectroscopy.* J. Am. Chem. Soc., 2008. **130**: p. 6310-6311.

29. Pielak, G.J., *Retraction: Protein dynamics in living cells.* Biochemistry, 2007. **46**(27): p. 8206.

30. Gajiwala, K.S., & Burley, S.K., *HDEA, a periplasmic protein that supports acid resistance in pathogeneic enteric bacteria.* J. Mol. Biol., 2000. **295**: p. 605-612.

31. Jackson, S.E., and Fersht, A.R., *Folding of chymotrypsin inhibitor 2. 1. Evidence for a two-state transition.* Biochemistry, 1991. **30**(43): p. 10428-35.

32. Hochstrasser, M., *Origin and function of ubiquitin-like proteins.* Nature, 2009. **458**: p. 422-429.

33. Bainer, R., Park, H., & Cluzel, P., *A High-throughput Capillary Assay for Bacterial Chemotaxis.* J. Microbiol. Methods, 2003. **55**: p. 315-319.

34. Delaglio, F., et al., *NMRPipe: A multidimensional spectral processing system based on UNIX pipes.* Journal of Biomolecular NMR, 1995. **6**(3): p. 277-293.

35. Johnson, B.A. and R.A. Blevins, *NMR View: A computer program for the visualization and analysis of NMR data.* Journal of Biomolecular NMR, 1994. **4**(5): p. 603-614.

36. Bryant, J.E., Lecomte, J.T., Lee, A.L., Young, G.B., and Pielak, G.J., *Protein dynamics in living cells.* Biochemistry, 2005. **44**: p. 9275-9279.

37. Sharaf, N.G., Barnes, C.O., Charlton, L.M., Young, G.B., & Pielak, G.J., *A Bioreactor for Protein In-Cell NMR.* J. Mag. Res., 2010. **202**(2): p. 140-146.

38. McNulty, B.C., et al., *Temperature-induced reversible conformational change in the first 100 residues of alpha-synuclein.* Protein Science, 2006. **15**(3): p. 602-608.

39. Charlton, L.M., et al., *Residue-level Interrogation of macromolecular crowding effects on protein stability.* Journal of the American Chemical Society, 2008. **130**(21): p. 6826-6830.

40. Ai, X., et al., *^{15}N NMR spin relaxation dispersion study of the molecular crowding effects on protein folding under native conditions.* Journal of the American Chemical Society, 2006. **128**(12): p. 3916-3917.

41. Homouz, D., et al., *Crowded, cell-like environment induces shape changes in aspherical protein.* proceedings of the National Academy of Sciences of the United States of America, 2008. **105**(33): p. 11754-11759.

42. Pielak, G.J., et al., *Protein nuclear magnetic resonance under physiological conditions.* Biochemsitry, 2009. **48**(2): p. 226-234.

43. Hartbrich, A., et al., *Development and application of a membrane cyclone reactor for in-vivo NMR spectroscopy with high microbial cell densities.* Biotechnology and Bioengineering, 1996. **51**(6): p. 624-635.

44. Majors, P.D., J.S. McLean, and J.C.M. Scholten, *NMR bioreactor development for live in-situ microbial functional analysis.* Journal of Magnetic Resonance, 2008. **192**(1): p. 159-166.

45. Dahan-Grobgeld, E., et al., *Reversible induction of ATP synthesis by DNA damage and repair in Escherichia coli. In-vivo NMR studies.* Journal of Biological Chemistry, 1998. **273**(46): p. 30232-30238.

46. Hesse, S.J.A., et al., *Measurement of intracellular (compartmental) pH by ^{31}P NMR in Aspergillus niger.* Journal of Biotechnology, 2000. **77**(1): p. 5-15.

47. Lang, A.E. and A.M. Lozano, *Parkinson's disease- first of two parts.* The New England Journal of Medicine, 1998. **339**(15): p. 1044-1053.

48. Serber, Z., et al., *Evaluation of parameters critical to observing proteins inside living Escherichia coli by in-cell NMR spectroscopy.* journal of the American Chemical Society, 2001. **123**(37): p. 8895-8901.

49. Bodenhausen, G. and D.J. Ruben, *Natural abundance nitrogen-15 NMR by enhanced heteronuclear spectroscopy.* Chemical Physics Letters, 1980. **69**(1): p. 185-189.

50. Kay, L., P. Keifer, and T. Saarinen, *Pure absorption gradient enhanced heteronuclear single quantum correlation spectroscopy with improved sensitivity.* Journal of the American Chemical Society, 1992. **114**(26): p. 10663-10665.

51. Schanda, P. and B. Brutscher, *Very fast two-dimensional NMR spectroscopy for real-time investigation of dynamic events in proteins on the time scale of seconds.* Journal of the American Chemical Society, 2005. **127**(22): p. 8014-8015.

52. Dulieu, C., D. Poncelet, and R.J. Neufeld, *Encapsulation and immobiliation techniques. In Cell encapsulation technology and therapeutics* W.M. Kuthreiber, R.P. Lanza, and W.L. Chick, Editors. 1999, Birkhauser: Boston p. 3-17.

53. Li, C., et al., *Differential dynamical effects of macromolecular crowding on an intrinsically disordered protein and a globular protein: implications for in-cell NMR spectroscopy.* Journal of the American Chemical Society, 2008. **130**(20): p. 6310-6311.

54. Slade, K.M., et al., *Effects of Recombinant Protein Expression on Green Fluorescent Protein Diffusion in Escherichia coli.* Biochemistry, 2009. **48**(23): p. 5083-5089.

55. Vieira, J. and J. Messing, *The pUC plasmids, an M13mp7-derived system for insertion mutagenesis and sequencing with synthetic universal primers.* Gene, 1982. **19**(3): p. 259-268.